PRAMANA
— journal of
physics

© Indian Academy of Sciences

Vol. 74, No. 5
May 2010
pp. 793–804

Harmonic dynamical behaviour of thallous halides

SARVESH K TIWARI[1,*], L J SHUKLA[2] and K S UPADHYAYA[3]
[1]Motilal Nehru National Institute of Technology, Allahabad 211 004, India
[2]Department of Physics, Raja Harpal Singh P.G. College, Singramau, Jaunpur 222 175, India
[3]Faculty of Science, Nehru Gram Bharti University, Nyay Nagar, Jhunsi, Allahabad 211 019, India
[*]Corresponding author. E-mail: sarvesh.tiwari@hotmail.com

MS received 6 November 2009; revised 19 January 2010; accepted 29 January 2010

Abstract. Harmonic dynamical behaviour of thallous halides (TlCl and TlBr) have been studied using the new van der Waals three-body force shell model (VTSM), which incorporates the effects of the van der Waals interaction along with long-range Coulomb interactions, three-body interactions and short-range second neighbour interactions in the framework of rigid shell model (RSM). Phonon dispersion curves (PDC), variations of Debye temperature with absolute temperature and phonon density of state (PDS) curves have been reported for thallous halides using VTSM. Comparison of experimental values with those of VTSM and TSM are also reported in the paper and a good agreement between experimental and VTSM values has been found, from which it may be inferred that the incorporation of van der Waals interactions is essential for the complete harmonic dynamical behaviour of thallous halides.

Keyword. Phonons; specific heat; infra-red spectra; Raman spectra.

PACS Nos 63.20.-e; 65.40.Ba; 78.30.-j

1. Introduction

The nature and the physical properties of the thallous halides have attracted an increased interest in the study of their lattice dynamics. Availability of the measured data on phonon dispersion curves [1,2], Debye temperature variations [3,4] along with their theoretical values [5], two-phonon IR and Raman spectra [6,7], elastic constants [1,8] and dielectric constants [9,10] of thallous halides (TlCl and TlBr) and their interpretations by means of theoretical models [11–17] with moderate success, have motivated the authors to develop a lattice dynamical model for the satisfactory description of their interesting properties.

The details of the progression for the study of phonon behaviour of thallous halides have been traced by several experimental and theoretical workers. The rigid ion model (RIM) of Kellermann [18] is the first important model, which considers

the ions of the crystal to be rigid, nondeformable and nonpolarizable spherical particles. The RIM could not interpret well the dynamical, optical and elastic properties. The next is the deformation dipole model (DDM) of Karo and Hardy [19] and rigid shell model (RSM) of Dick and Overhauser [20] and Woods *et al* [21] by two different groups of workers. The DDM allows only the redistribution of charges in deformed electron cloud while the shell model considers the relative displacement. So both effects (deformation and displacement) are present in ionic crystals. A general way to remove this deficiency is to include the deformation of electron shells in the framework of RSM. The most prominent amongst them are breathing shell model (BSM) of Schroder [22], the deformable shell model (DSM) of Basu and Sengupta [23] and three-body force shell model (TSM) of Verma and Singh [24].

Further, Singh *et al* [25] used the extended three-body force shell model (ETSM) which is an amalgamation of RSM and DDM. ETSM contains (i) the two-body long-range Coulomb interaction and short-range repulsion effective up to the second-neighbour ions, (ii) the long-range three-body forces and (iii) the dipole character of the constituent ions. Despite their success, ETSM has some features which do not have much physical significance.

The experimental and theoretical workers have, however, advised that their results can be further improved by considering the van der Waals interaction effect. Recently, Upadhyaya *et al* [26] have obtained better results between theory and experiment for ionic semiconductors using van der Waals interaction. This has motivated the author to incorporate the effects of van der Waals interactions and three-body interactions in the framework of ion polarizable RSM with short-range interactions effective up to the second neighbour. Therefore, it may be inferred that the most realistic model for complete harmonic dynamical behaviour of the crystals under consideration can be developed by introducing the effect of van der Waals interactions (VWI) and three-body interactions (TBI) in the framework of RSM. The present model is known as van der Waals three-body force shell model (VTSM) and has the following broad features:

(i) The number of model parameters obtained for each crystal is twelve.
(ii) The same input data (physical properties) are used for the computation of parameters for each crystal.
(iii) The element of VWI has been added to the short-range repulsive interactions operative up to the second neighbours.
(iv) Efforts have been made to keep the computation completely objective without any bias.

2. Theory

The van der Waals interaction potential owes its origin to the correlations of the electron motions in different atoms. The electrons of each atom shift with respect to the nucleus in the presence of other atoms and consequently an atom becomes an electric dipole. The instantaneous dipole moment of a closed shell atom induces

dipole moment on a similar atom and the interaction energy thus arising is known as the van der Waals (VW) interaction potential.

The necessity of including the van der Waals interaction (VWI) and three-body interaction (TBI) effects in the framework of rigid shell model (RSM) [21] has already been discussed above. The aim of this section is, therefore, to give a detailed account of the essential formalism of the present lattice dynamical model, the VTSM. Thus, the inclusion of VWI and TBI effects in RSM will employ the Hietler–London and the free-electron approximations. The interaction systems of the present model thus consist of the long-range screened Coulomb, van der Waals interactions, three-body interactions and the short-range overlap repulsion operative upto the second-neighbour ions in thallous halides.

The general formalism of VTSM can be derived from the crystal potential whose relevant expression per unit cell is given by

$$\Phi = \Phi^{\mathrm{C}} + \Phi^{\mathrm{R}} + \Phi^{\mathrm{TBI}} + \Phi^{\mathrm{VWI}}, \tag{1}$$

where Φ^{C} is the Coulomb interaction potential, Φ^{R} is the short-range overlap repulsion potential, Φ^{TBI} is the three-body interaction potential and Φ^{VWI} is the van der Waals interaction potential.

Using the crystal energy expression (1) the equations of motion of two cores and two shells can be written as

$$\omega^2 MU = (R + Z_m C' Z_m)U + (T + Z_m C' Y_m)W, \tag{2}$$

$$O = (T^T + Y_m C' Z_m)U + (S + K + Y_m C' Y_m)W. \tag{3}$$

Here, U and W are vectors describing the ionic displacements and deformations respectively, Z_m and Y_m are the diagonal matrices of modified ionic charges and shell charges, respectively, M is the mass of the core, T and R are the repulsive Coulombian matrix respectively; C' and Y_m are the long-range interaction matrix which includes Coulombian and three-body interaction respectively; S and K are core–shell and shell–shell repulsive interaction matrices respectively and T^{T} is the transpose of the matrix T. All these variables are as described in [21].

The introduction of VWI and TBI in the framework of RSM with the elimination of W from eqs (2) and (3) leads to the secular determinant:

$$|D(\vec{q}) - \omega^2 MI| = 0. \tag{4}$$

Here $D(q)$ is the (6×6) dynamical core–core repulsive interaction matrix given by

$$\begin{aligned} D(\vec{q}) = {} & (R' + Z_m C' Z_m) - (T + Z_m C' Y_m) \\ & \times (S + K + Y_m C' Y_m)^{-1} (T^{\mathrm{T}} + Y_m C' Z_m). \end{aligned} \tag{5}$$

The number of adjustable parameters has been largely reduced by considering all the short-range interactions to act only through the shells. This assumption leads to $R = T = S$. The expressions for the second-order elastic constants (C_{11}, C_{12} and C_{44}) derived from the dynamical matrix corresponding to the VTSM are

$$C_{11} = \frac{e^2}{4a^4}\left[0.7010 Z_m^2 + \frac{A_{12} + 2B_{12}}{6} + \frac{A_{11} + A_{22}}{4} + 5.4283\xi'^2\right]. \tag{6}$$

$$C_{12} = \frac{e^2}{4a^4}\left[-0.6898Z_m^2 + \frac{A_{12} - 4B_{12}}{6} - \frac{B_{11} + B_{22}}{4} + 5.4283\xi'^2\right] \quad (7)$$

$$C_{44} = \frac{e^2}{4a^4}\left[-0.3505Z_m^2 + \frac{A_{12} + 2B_{12}}{6} + \frac{B_{11} + B_{22}}{4}\right]. \quad (8)$$

In view of the equilibrium condition $((\mathrm{d}\Phi/\mathrm{d}r)_0 = 0)$ we obtain

$$B_{11} + 2B_{12} + B_{22} = -0.6786Z_m^2 \quad (9)$$

where

$$Z_m^2 = Z^2\left(1 + \frac{16}{Z}f_0\right) \quad \text{and} \quad \xi'^2 = Zr_0f_0' \quad (10)$$

$f_0' = (\mathrm{d}f/\mathrm{d}r)_{r=r_0}, r_0 = a\sqrt{3}$ is the interionic separation.

The term f_0 is a function dependent on the overlap integrals of the electron wave functions and the subscript zero indicates the equilibrium value.

These elastic constants lead to the Cauchy violation

$$C_{12} - C_{44} = e^2/4a^4(5.4283Zr_0f_0'). \quad (11)$$

By solving the secular eq. (2) along [q 0 0] direction and subjecting the short- and long-range coupling coefficients to the long-wavelength limit $\vec{q} \to 0$, the expression for zone centre optical vibration frequencies are given by

$$(\mu\omega_L^2)_{q=0} = R_0' + \frac{(Z'e)^2}{vf_L} \cdot \frac{8\pi}{3}(1 + 12Z_m^{-2}Zr_0f_0') + W_0 \quad (12)$$

$$(\mu\omega_L^2)_{q=0} = R_0' - \frac{(Z'e)^2}{vf_L} \cdot \frac{4\pi}{3} + W_0 \quad (13)$$

where

$$R_0' = R_0 - e^2\left(\frac{d_1^2}{\alpha_1} + \frac{d_2^2}{\alpha_2}\right); \quad Z' = Z_m + d_1 - d_2 \quad (14)$$

$$f_L = 1 + \frac{8\pi\alpha}{3v}(1 + 12Z_m^{-2}Zr_0f_0') \quad (15)$$

$$f_T = 1 - \frac{4\pi\alpha}{3v} \quad (16)$$

and

$$\alpha = \alpha_1 + \alpha_2. \quad (17)$$

W_0 is the van der Waals interaction term.

3. Computations

Model parameters for thallous halides have been computed for VTSM as detailed above from the known experimental values of the equilibrium interatomic separation (r_0), elastic constants (C_{11}, C_{12} and C_{44}), polarizabilities (α_1, α_2), dielectric constants (ε_0, ε_∞) and frequencies [$\nu_{\mathrm{TO}}(\Gamma)$, $\nu_{\mathrm{LO}}(\Gamma)$, $\nu_{\mathrm{LO}}(R)$, $\nu_{\mathrm{LA}}(R)$, $\nu_{\mathrm{TO}}(X)$ and $\nu_{\mathrm{TA}}(X)$].

These model parameters are used to compute the phonon spectra for the 56 allowed nonequivalent wave vectors in the first Brillouin zone and the frequencies along the symmetry directions have been plotted to obtain the phonon dispersion curves (PDCs). These curves have been compared with the curves measured [1,2] by means of coherent inelastic neutron scattering technique. As the neutron scattering experiments provide the data along the symmetry directions only, studies on the Debye temperature variations and two-phonon density of states (PDS) have also been carried out for the complete description of the frequencies for the Brillouin zone. The specific heat C_{v} has been computed at different temperatures using Blackman's [27] sampling technique and the corresponding values of Θ_{D} have been plotted against the absolute temperature (T) and have also been compared with the available experimental data [3,4].

The phonon spectra have been used to calculate the phonon density of states (PDS), $N(\nu_j + \nu_{j'})$ corresponding to the sum modes $(\nu_j + \nu_{j'})$, following the procedure of Smart *et al* [28]. A histogram between $N(\nu_j + \nu_{j'})$ and $(\nu_j + \nu_{j'})$ is plotted and smoothed out to obtain the PDS curves. These curves show well-defined peaks which correspond to two-phonon infra-red/Raman scattering peaks and peaks have been compared with the observed peaks [6,7]. As the division of the Brillouin zone in the present case is somewhat coarse, the fine structure of the infra-red/Raman shifts may not be reproduced completely. To interpret them, the critical point analysis has been used following the method prescribed by Burstein and Lax [29].

The overall computed results for thallous halides (TlCl and TlBr) are presented in the following section.

4. Results and discussion

Input data along with the relevant references for TlCl and TlBr are presented in table 1 and the model parameters calculated using VTSM and TSM [12] are given in table 2. These model parameters have been used to calculate the complete phonon dispersion frequencies in the first Brillouin zone. These frequencies have, in turn, been used to compute the variations of Debye temperatures with specific heats. The observed infra-red/Raman spectra have also been interpreted with the help of phonon density of state (PDS) approach and critical point analysis, using the above spectrum. Phonon dispersion curves (PDCs) along the principal symmetry directions, Debye temperature variations and phonon density of state (PDS) curves for these crystals using VTSM are plotted in figures 1, 2 and 3, respectively, along with respective experimental values for visual comparison. Figure 4 presents a visual comparison of PDCs with VTSM, TSM and the experimental values along the principal symmetry directions for TlBr, but the visual comparison of PDCs

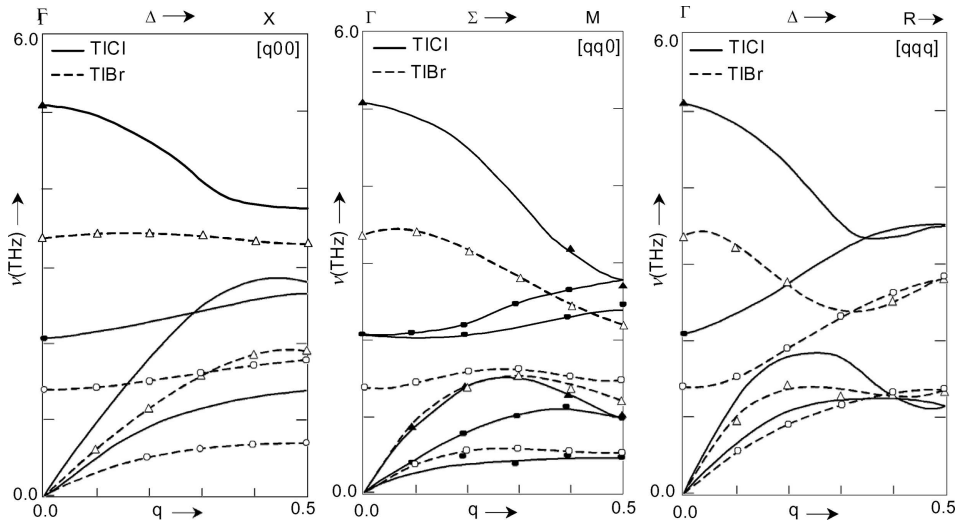

Figure 1. Phonon dispersion curves of TlCl and TlBr. *Experimental points*: TlCl [1]: (▲) Longitudinal, (●) transverse. TlBr [2]: (△) Longitudinal, (○) transverse. *Present study (VTSM)*: (—) TlCl, (- - -) TlBr.

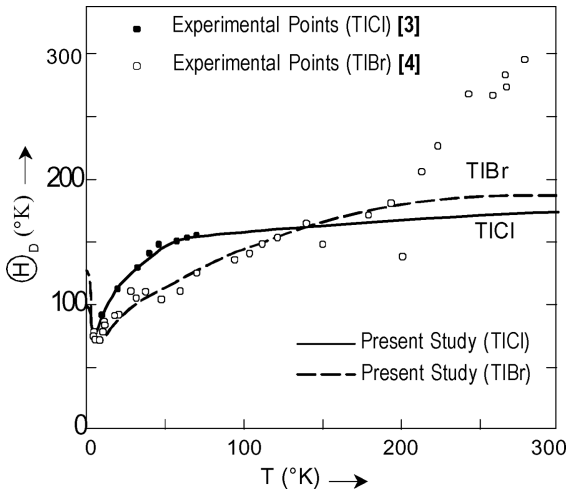

Figure 2. Debye temperature variations for TlCl and TlBr.

could not be drawn for TlCl due to the nonavailability of the data for the TSM. The VTSM assignments of infra-red/Raman peaks for these crystals using critical point analysis are listed in tables 3 and 4 and plotted with experimental peaks [6,7] in figure 3. Quantitative comparison of frequencies along the principal symmetry directions of the measured PDCs [1,2] and those reported from VTSM and TSM [12] as well as experimental values are presented in table 5.

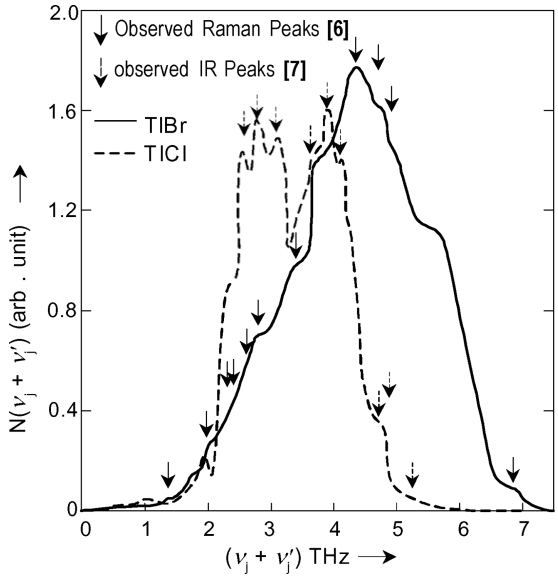

Figure 3. Phonon density of state curves for TlBr and TlCl.

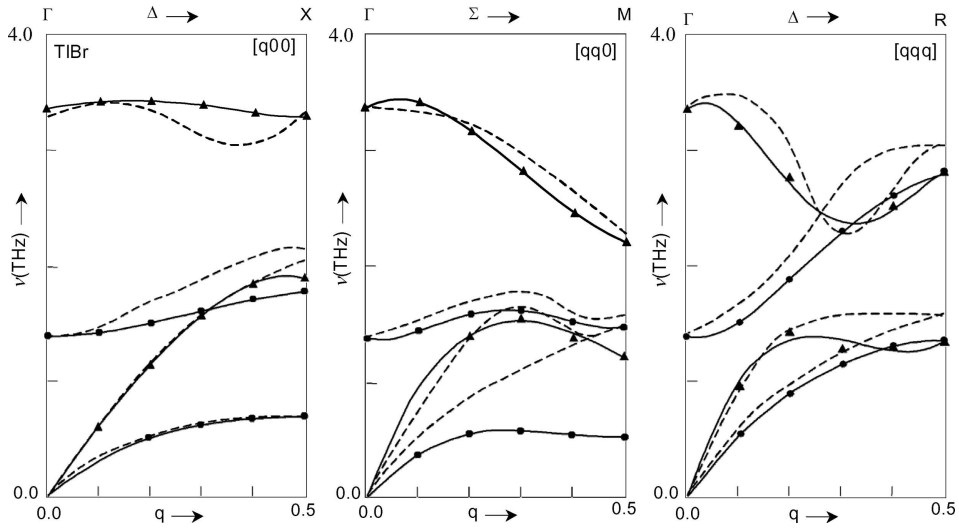

Figure 4. Comparative phonon dispersion curves for TlBr with VTSM and TSM. Experimental points [2]: (▲) Longitudinal, (•) transverse. (—) VTSM, (- - -) TSM [12].

From figure 1 it is evident that in the phonon dispersion curves (PDCs), three-body interactions have influenced both longitudinal and transverse optical as well as acoustic branches of the crystals under consideration. Another noteworthy feature of the present model is the excellent reproduction of almost all the acoustic

Table 1. Input data for TlCl and TlBr [C_{ij} (in 10^{12} dyne/cm^2), ν (in THz), r_0 (in 10^{-8} cm), α_i (in 10^{-24} cm^3)].

	TlCl		TlBr	
Constants	Values	Ref.	Values	Ref.
C_{11}	4.690	[8]	4.399	[10]
C_{12}	1.740	[8]	1.660	[10]
C_{44}	1.080	[8]	1.079	[10]
$\nu_{\mathrm{TO}}(\Gamma)$	2.080	[30]	1.390	[1]
$\nu_{\mathrm{LO}}(\Gamma)$	5.070	[30]	3.270	[–[a]]
$\nu_{\mathrm{LO}}(R)$	2.340	[30]	2.870	[1]
$\nu_{\mathrm{LA}}(R)$	1.140	[30]	1.350	[1]
$\nu_{\mathrm{TO}}(X)$	1.690	[30]	1.830	[1]
$\nu_{\mathrm{TA}}(X)$	1.040	[30]	0.650	[1]
α_1	4.800	[31]	5.100	[31]
α_2	2.927	[31]	4.125	[31]
ε_0	37.600	[30]	32.500	[10]
ε_∞	5.000	[30]	5.860	[10]
$2a$	3.678	[32]	3.948	[1]

[a]Calculated using LST relation.

Table 2. Model parameters for TiCi and TlBr.

TlCl		TlBr			
VTSM		VTSM		TSM [12]	
Properties	Values	Properties	Values	Properties	Values
Z_m^2	0.5552	Z_m^2	0.6858	A	3.6123
$r_0 f_0'$	0.02406	$r_0 f_0'$	0.02818	B	−0.2327
A_{11}	−0.4235	A_{11}	−3.0512	d_{m1}	0.1200
B_{11}	−2.2393	B_{11}	−0.0421	d_{m2}	0.1550
A_{12}	11.5052	A_{12}	10.6423	Y_{m1}	−5.0800
B_{12}	−0.5650	B_{12}	−0.5384	Y_{m2}	−3.1760
A_{22}	2.7131	A_{22}	1.6915	f_0	−0.0196
B_{22}	−2.4696	B_{22}	−2.0687	$r_0 f_0'$	0.0282
d_1	0.8623	d_1	0.7318		
d_2	0.9716	d_2	0.9156		
Y_1	−3.1004	Y_1	−2.8889		
Y_2	−1.6779	Y_2	−1.8676		

branches. The agreement achieved from the present model is also excellent for the LA, TA and LO branch along [q q 0] direction. This may be particularly because the zone centre vibration frequencies have been used as input data in the calculation of model parameters. A quantitative interpretation of the general features of PDC is also obvious from the present model when it predicts the gap between the

Table 3. Assignments of infra-red peaks for TlCl.

	Infra-red active			
PDS peaks (cm^{-1})	Observed [6] peaks (cm^{-1})	Present study		
		Assignment	Values (cm^{-1})	Deviation from the observed values (cm^{-1})
35	–	2TA(M)	34	–
69	–	2LA(M)	70	–
128	–	LO + LA(M)	128	–
155	–	LO + LA(R), LO + TA(R) TO + LA(R), TO + TA(R)	155	–
167	168	–	–	–
183	184	2LO(M)	186	2
207	–	–	–	–
247	249	–	–	–
257	255	–	–	–
273	272	–	–	–
313	315	–	–	–
–	350	–	–	–

Table 4. Comparative assignments of two-phonon Raman peaks from VTSM and TSM for TlBr.

	Raman active					
			Present study		TSM [12]	
PDS peaks (cm^{-1})	Observed [7] peaks (cm^{-1})	Assignment	Values (cm^{-1})	Deviation from the observed values (cm^{-1})	Values (cm^{-1})	Deviation from the observed values (cm^{-1})
45	43	LO(X) – LA(X)	46	3	–	–
59	–	LA(M) + TA(M)	60	–	–	–
68	66	LA(M) + TO(M)	68	2	–	–
95	93	LO(M) + TA(M)	93	0	85	8
115	113	LO(M) + LA(M)	117	4	–	–
125	123	LO(M) + TO(M)	125	2	115	8
150	156	2LO(M)	150	6	–	–
186	–	2LO(R)	186	–	–	–
226	229	2LO(Γ)	224	5	–	–

acoustical and optical branches similar to the forbidden gap between the valence and the conduction bands.

From table 5, it is observed that in the case of TlCl, the percentage deviation of frequencies for VTSM from the experimental values is maximum for optical branch (TO) along the M-symmetry direction, which is 2.83%, and deviation for the LO

Table 5. Deviation of experimental frequencies with VTSM and TSM along principal symmetry directions for TlBr.

		VTSM			TSM		
		Symmetry direction					
Crystal	Branch	X (%)	M (%)	R (%)	X (%)	M (%)	R (%)
TlCl	LO	–	2.56	–	–	–	–
	TO	–	2.83	–	–	–	–
	LA	–	0.00	–	–	–	–
	TA	–	0.00	–	–	–	–
TlBr	LO	0.30	0.00	1.07	1.82	1.36	8.57
	TO	0.00	0.67	1.07	18.99	6.67	8.57
	LA	2.60	1.23	5.30	5.73	20.16	25.00
	TA	0.29	1.85	5.30	0.29	20.16	25.00

branch along the M-symmetry direction is 2.56%, whereas no deviation is observed for both the acoustic branches (LA and TA) along the M-symmetry direction. Due to the nonavailability of experimental values for the X- and R-symmetry directions, deviation between the experimental values with those calculated using VTSM could not be obtained. Thus, the overall percentage deviation between the experimental and VTSM values along all the directions is within 2.83%. In the case of TlBr, the percentage deviation between experimental and VTSM values of frequencies is maximum for both the acoustic branches (LA and TA) along the R-symmetry direction, whereas no deviation could be observed along the optical branches (TO) along X-symmetry direction and LO along M-symmetry direction. On the other hand, the percentage deviation of frequencies for the model TSM from the experimental values is maximum for both the acoustic branches along the R-symmetry direction, which is 25%, whereas the minimum deviation is along the TA(X) branch, which is 0.29% and the deviation along all the directions is within 25%. Therefore, from the above analysis it could be inferred that the VTSM values are very close to the experimental values when compared to the TSM values and thus our model is very close to the measured phonon dispersion curves (PDCs) of TlBr along all the points, i.e. X, M and R for both optical as well as acoustic branches. Quantitatively, the agreement achieved from our present model is comparatively better in the sense that some of the fitted parameters by other workers [11–17], have attained unrealistic values. Moreover, we have tested the adequacy of the present model by calculating the Debye temperature variations, two-phonon Raman and anharmonic elastic properties.

The variations of Debye temperatures (Θ_D) with the temperature (T) are shown in figure 2 for these halides. The calculated Θ_D–T curves for TlCl and TlBr are in excellent agreement with the experimental [3,4] and theoretical [5] results calculated using shell model. Though the agreement is almost better with our model, VTSM, there is a slight discrepancy between theoretical and experimental results at higher temperatures which can be due to the exclusion of the effect of

anharmonicity in the present model. The success of the present model in exploring the specific heat indicates its adequacies to describe the lower range of frequency spectra. This is not surprising because the present model is quite capable to explain the elastic constants and hence the acoustic frequencies in terms of three-body interactions.

The two-phonon infra-red (IR) and Raman spectra are sensitive to the higher frequency side of the phonon spectra and the specific heats are sensitive to its lower side. It seems, therefore, essential to investigate the extent to which the present model is capable to interpret the Raman and IR spectra. This will provide a complete test for the validity of the present model for the entire range of the spectra. The results of these investigations from PDS approach listed in tables 3 and 4 and depicted in figure 3 show that the agreement between experimental [6,7] and our theoretical peaks is very good for infra-red/Raman spectra of TlCl and TlBr. As our PDS curves are derived from somewhat course mesh division of the Brillouin zone, we have used a critical point analysis [27] to present complex interpretation of the observed infra-red and Raman spectra. The assignments made by the present study along with those obtained from the TSM [12] listed in tables 3 and 4 for TlCl and TlBr respectively, show reasonably good agreement with the observed peaks corresponding to infra-red/Raman spectra of these halides. Our extensive study of two-phonon infra-red/Raman spectra is basically aimed to correlate the theoretical and optical experimental results. The interpretation of Raman spectra achieved from both PDS approach and critical point analysis may be considered satisfactory in all cases. These predictions can be improved further by using a sophisticated programme [28], for generating the phonon density of states. A successful interpretation of these spectra has provided the next best test of any model for higher range of frequency spectra.

5. Conclusion

From the above discussion, it may be concluded that our model provides a good agreement between theoretical and experimental results and is certainly better than the results obtained by means of theoretical models [11–17]. Therefore, it may be inferred that the inclusion of van der Waals interaction is very essential for the complete description of the phonon dynamical behaviour of crystals with CsCl structure.

Acknowledgement

The authors are grateful to the Principal, K.N. Government P.G. College, Gyanpur, SRN Bhadohi (India) for providing the necessary facilities. The authors are also thankful to the Computer Centre, BHU, Varanasi (India) for providing computational assistance.

References

[1] Y Fuzi, *J. Phys. Soc. Jpn* **44**, 1237 (1978)
[2] E R Cowley and A Okazaki, *Proc. R. Soc. London* **A300**, 45 (1965)

[3] A D Redaumond and B Yates, *J. Phys.* **C5**, 1589 (1972)
[4] R M Brade and B J Yates, *J. Phys.* **C4**, 417 (1971)
[5] R Kamal and R G Mandiratta, *J. Phys. Soc. Jpn* **26**, 621 (1969)
[6] M Krauzmann, *C.R. Acad. Sci. (France)* **B268**, 14 (1969)
[7] J M Brom Jr and H F Frazen, *J. Chem. Phys.* **54**, 2874 (1971)
[8] S Hausshal, *Phys. Rev.* **165**, 959 (1968)
[9] R P Lowndes and D H Martin, *Proc. R. Soc. London* **A308**, 473 (1969)
[10] G E Morse and A W Lawson, *J. Phys. Chem. Solids* **26**, 939 (1969)
[11] H N Gupta and R S Upadhyaya, *Phys. Status Solidi* **B93**, 781 (1979)
[12] H N Gupta and R S Upadhyaya, *Phys. Status Solidi* **B102**, 143 (1980)
[13] H H Lal, *Three-body forces and lattice dynamics of halides of some heavy monovalent metals*, Ph.D. Thesis (Banaras Hindu University, 1971) Unpublished
[14] R K Singh and H N Gupta, *Proc. R. Soc. London* **349**, 289 (1976)
[15] Vipasha Mishra, S P Sanyal and R K Singh, *Phil. Mag.* **A55**, 583 (1981)
[16] R K Singh, H N Gupta and S P Sanyal, *IL Nuovo Cemento* **60**, 89 (1980)
[17] H H Lal and M P Verma, *J. Phys.* **C5**, 543 (1972)
[18] E W Kellarmann, *Phil. Trans. Roy. Soc. (London)* **A238**, 513 (1940); *Proc. Roy. Soc.* **A178**, 17 (1941)
[19] A M Karo and J R Hardy, *J. Chem. Phys.* **48**, 3173 (1968)
[20] B G Dick and A W Overhauser, *Phys. Rev.* **112**, 90 (1958)
[21] A D B Woods, W Cochran and B N Brockhouse, *Phys. Rev.* **119**, 980 (1960)
[22] U Schroder, *Solid State Commun.* **4**, 347 (1966)
[23] A N Basu and S Sengupta, *Phys. Status Solidi* **29**, 367 (1968)
[24] M P Verma and R K Singh, *Phys. Status Solidi* **33**, 769 (1969); **36**, 335 (1969); **38**, 851 (1970)
[25] R K Singh, H N Gupta and M K Agrawal, *Phys. Rev.* **B17**, 894 (1978)
[26] K S Upadhyaya, M Yadav and G K Upadhyaya, *Phys. Status Solidi* **B229**, 1129 (2002)
[27] M Blackmann, *Z. Phys.* **82**, 421 (1933); *Trans. Roy. Soc.* **A236**, 102 (1955)
[28] C Smart, G R Wilkinson, A M Karo and J R Hardy, *Lattice dynamics* edited by R F Wallis (Pergamon Press, Oxford, 1965)
[29] E Burstein and M Lax, *Phys. Rev.* **97**, 39 (1955)
[30] R P Lowndes and D H Martin, *Proc. R. Soc. London* **A308**, 473 (1969)
[31] J R Tessman, A Kahn and W Schokley, *Phys. Rev.* **92**, 890 (1953)
[32] R Z Bachrach and F C Brown, *Phys. Rev.* **B1**, 818 (1970)